24th COBEM - 2017

24th ABCM International Congress of Mechanical Engineering
December 3-8, 2017, Curitiba, PR, Brazil

COBEM-2017-5949
STRESS ANALYSIS OF A DIFFUSION BONDING DEVICE UNDER LOADING AND THERMAL EXPANSION

Gabriel Serafin Couto Vieira
Gustavo George Verdieri Nuernberg
Universidade Federal de Santa Catarina, Florianópolis, Brazil
gabriel.serafin@labtucal.ufsc.br
verdieri@labtucal.ufsc.br

Nelson Yurako Londoño Pabón
Universidade Federal de Santa Catarina, Florianópolis, Brazil
nelson@labtucal.ufsc.br

Marcia Henriques Barbosa Mantelli
Universidade Federal de Santa Catarina, Florianópolis, Brazil
marcia.mantelli@labtucal.ufsc.br

Abstract. *The process of diffusion bonding occurs when two solid mating surfaces join through the atomic diffusion of their solid bodies. While temperature, pressure and time are the fundamental diffusion bonding process parameters, its effectiveness also depends on the geometrical properties of the bodies. In order to provide appropriate pressure distribution to these mating surfaces, a device was proposed. It consists of two stainless steel boards with passing holes near its edges and carbon steel screws to provide the needed pressure. The samples to be bounded consist of slabs of aluminum and are sandwiched between the boards. Screws hold the whole system tightly together while the set is subjected to high temperatures. It is noted that the aluminum's coefficient of thermal expansion is significantly larger than that of the stainless and carbon steels. Therefore, when subjected to temperature variations, the previously calculated pressure does not stand and, therefore, the temperature effects on the thermal expansions and on the Young's module, must be considered in the determination of the applied pressure. Moreover, previous experience shows that the indiscriminate use of pressure may irreparably damage the pressure application device during the bounding process. The purpose of this work is to provide a solid mechanic study of the stress distribution observed in the pressure device, while it is subjected to high temperatures and loads, during the diffusion bonding process. Special attention is given to the estimative of the real pressure while heating takes place.*

Keywords: *Diffusion bonding, stress analysis, thermal expansion.*

1. INTRODUCTION

Diffusion bonding is a joining process, where the principal mechanism is the inter-diffusion of atoms across the bonding interface (Kazakov, 1985). In theory, as stated by Pavlova (2005), if two ideally plane and clean metallic surfaces were to be put in contact, a bond would naturally occur. This would be due to the proximity between the atoms and due to the formation of chemical bonds between the molecules. However, given the impossibility to remove surface roughness, such conditions are impossible to obtain in practical terms.

According to Mortean (2014), temperature, external pressure and time are fundamental process parameters for diffusion bonding. The high temperature activates the process while the external pressure guaranties the intimate contact between the mating surfaces.

It should be noted, however, that in this process, the fusion temperature is not reached. The required temperature for the bonding is around fifty to eighty percent of the absolute fusion temperature of the material. At the same time, several mechanical properties, such as Young's Modulus and Yield Strength, are affected negatively by higher temperatures. Therefore, the geometry and the materials of the pressurizing system must be carefully selected, so that the device can withstand the imposed pressure during the bonding process.

One of the most advanced devices available for diffusion bonding are hot press furnaces. In order to preserve the steadiness of process parameters, they count with active control of temperature and pressure. Figure 1 depicts the interior

of a hot press furnace, with hydraulic pistons to provide pressure and an array of electrical resistances to provide the needed heat.

These features make them the most appropriate devices for diffusion bonding. However, the use of these devices has its technical restrains, as they present high rates of energy consumption, high operational costs, time-consuming cycles and are very sensitive to contamination.

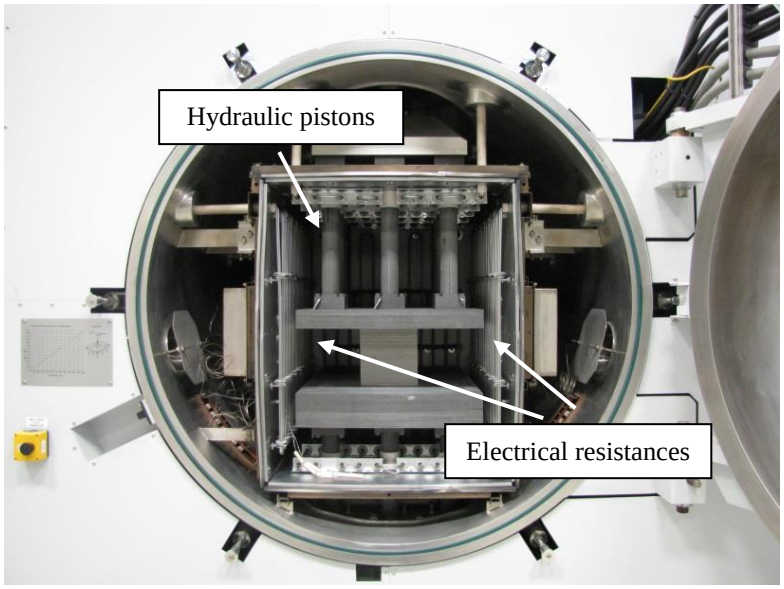

Figure 1. Interior of a hot press furnace (PVA Tepla MOV 653 HP in Heat Pipe Laboratory/UFSC) with active pressure control.

On the other hand, the possibility of using simpler diffusion bounding methods, especially in the initial phases of project development, is appealing. The Heat Pipe Laboratory/UFSC counts with a PVA Tepla MOV 653 HP hot press furnace. However, when the use of such equipment is not possible, mechanical press apparatuses, similar to the one depicted in Figure 2 have proven to function with satisfactory results.

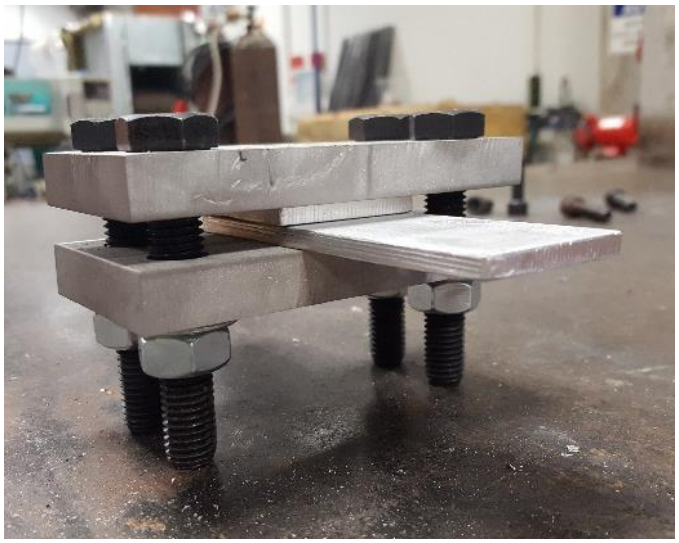

Figure 2. Example of alternative pressure-applying device used in first stages of diffusion bonding experiments.

The purpose of applying high pressure is to force intimate contact between adjoining surfaces. It was noted, however, that the temperature heavily influences the resistance of these simple pressurizing systems. In extreme cases, the device may be irreversibly distorted. Further use of the mechanism is restricted if its parallelism is hampered during a diffusion bounding cycle. The objective of the present work is to study the influence of the sintering temperature over the mechanical behavior of the pressure-applying device.

2. STRESS ANALYSIS

The studied pressure-applying device is composed of two rectangular stainless steel boards. They were machined with help of a water jet cutter. Its dimensions are: 110 *mm* in length, 55 *mm* in width and 13.1 *mm* in thickness. Each one of these boards has four passing holes near its corners. These holes have 13 *mm* of diameter and their centers are 14.5 *mm* away from the borders. The dimensions are depicted in Figure 3.

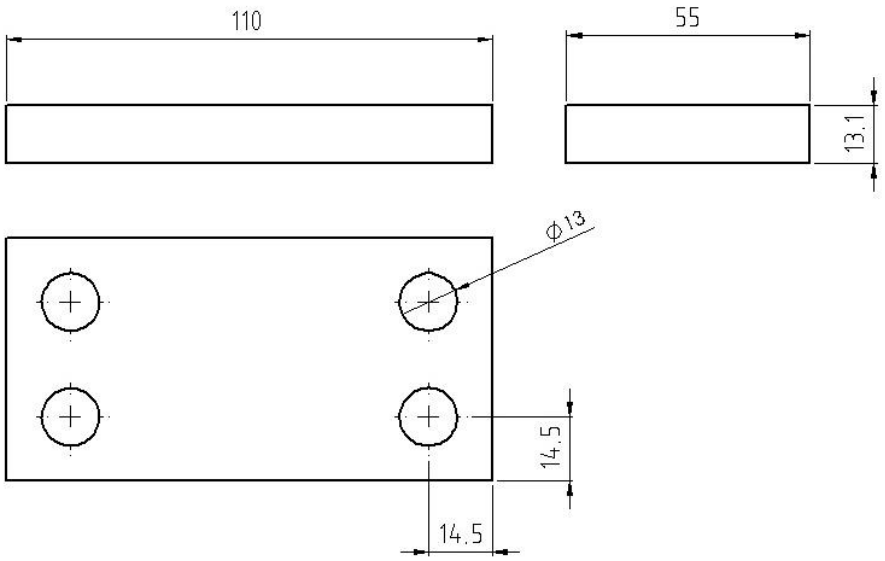

Figure 3. Dimensions of the stainless steel board.

The specimens to be bounded are composed of aluminum slabs. They present 5 *mm* thickness and were grinded with a grindstone and then with a round wire brush. Afterwards, grit size 120 sandpaper was used to provide the superficial finishing. The slabs are positioned on the device so that the affected area measures 36 x 44 mm^2. M12 screws are used to provide the pressure. Equation 1 relates the screw axial force with the torque applied on the screw head, where the symbols are explained in Table 1 (Norton, 2006). For a pressure of 10 *MPa*, the required force on each one of the screws is 3960 *N*.

$$T \cong F\frac{d_m}{2}\left[\left(\frac{\mu+\tan\lambda\cos\alpha}{\cos\alpha-\mu\tan\lambda}\right)+\mu_c 0.625\right], \tan\mu=\frac{l}{\pi d_m} \tag{1}$$

Table 1. Physical meaning of the used symbols.

Symbol	Physical meaning	Measurement Unit
T	Torque on the screws head	*N.m*
F	Force on the screw axis	*N*
d_m	Nominal diameter	*m*
μ	Thread coefficient of attrition	-
α	Thread angle	°
λ	Lead angle	°
μ_c	Screw's collar coefficient of attrition	-
l	Lead	*m*
π	Pi (Mathematical constant)	-

After the device was assembled, the set is placed inside a tubular oven with hydrogen atmosphere. The heating cycle presents a heating slope of 10 *°C/min*, until reaching temperatures of 550 *°C*. The oven temperature rises steadily and over a relatively long period of time. Therefore, in terms of modelling, also considering the much larger size of the oven, steady state conditions are assumed for the bounding boards at all times.

The thermal expansion coefficient is an important physical property that predicts the elongation caused by temperature changes. For this study, the thermal expansion coefficients were obtained from a specialized website (Matweb, 2017). Table 2 shows these properties for the materials involved in the present work.

Table 2. Thermal expansion (α) coefficients for different temperatures.

Temperature interval [°C]	$\alpha_{CarbonSsteel}$ [$\mu m/m°C$]	$\alpha_{StainlessSteel}$ [$\mu m/m°C$]	α_{Al} [$\mu m/m°C$]
$20 < \Delta T < 100$	10.1	16	24
$100 < \Delta T < 300$	13.5	19.9	25.5
$300 < \Delta T < 600$	16.6	19.9	27.4

Spline adjustment curves correlate the thermal expansion coefficients for each material. The resulting expressions were used to predict the behavior of this property as a function of the temperature:

$$\alpha_{CarbonSteel} = -2\,10^{-5}T^2 + 0.0113T + 11.731 \tag{2}$$

$$\alpha_{StainlessSteel} = 6\,10^{-6}T^2 - 0.0008T + 16.128 \tag{3}$$

$$\alpha_{Al} = -4\,10^{-6}T^2 + 0.0116T + 23.314 \tag{4}$$

The elongation (dilatation δ) due to the thermal expansion coefficient and temperature gradient can be predicted by the equation:

$$\delta = \alpha l_o \Delta T \tag{5}$$

where l_o is the original length (l_{slab}=5 *mm*, l_{board}=13.1 *mm* and l_{screw}=18,1 *mm*) and ΔT, the change in temperature. The expected dilatation curves for the component materials of the set up under study and the heating slope are given in Figure 4.

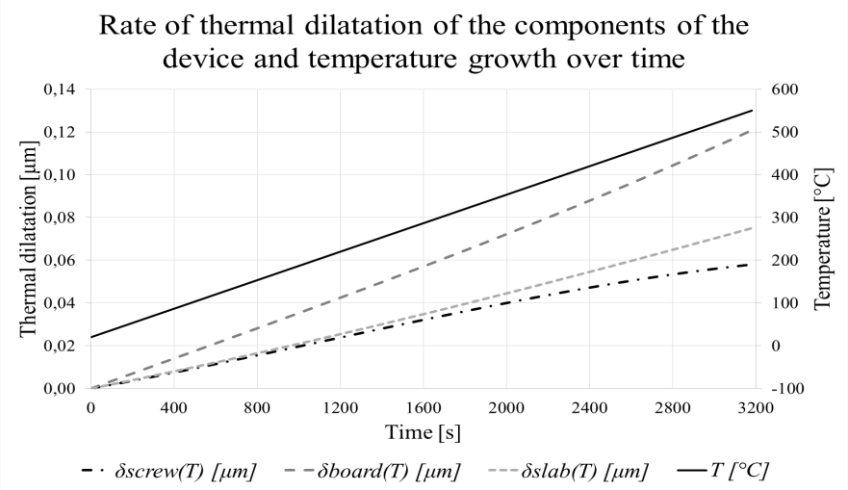

Figure 4. Estimated thermal deformation of the different specimens during test.

It should be noted that the expected thermal dilatation of the aluminum slabs and of the stainless steel boards are larger than those of the carbon steel screws. As the screws force the device to stay in their original position, the net value of the expansion of the components will result in a deformation of the set up components. This deformation, in turn, will result in different values of the pressure applied on the aluminum slabs.

The change in Young's Moduli of the materials over the temperature change is another important aspect to be considered. It is expected that it will be very important part while recalculating the pressure on the slabs. Under the assumption that the components of the device may be modelled as linear springs, the following equation can be used to calculate the equivalent spring constant for both the screw and the slab:

$$k_{screw,slab} = \left(\frac{EA}{h} \right)_{screw,slab} \tag{6}$$

where A is the area perpendicular to the applied force, *h* is the length in the direction of the force and E is the Young's Modulus.

For the screws, the tensile stress area is calculated with the following equations (Budynas and Nibsbett, 2011):

$$A_t = \frac{\pi}{4}(d_t)^2 \tag{7}$$

$$d_t = \frac{d_p + d_r}{2} \tag{8}$$

$$d_p = d - 0.649519p \tag{9}$$

$$d_r = d - 1.226869p \tag{10}$$

where A_t is the tensile stress area, d_t, the tensile diameter, d_p, the pitch diameter, d_r, the minor diameter and p, the pitch. Collectively, the area of the four screws amounted 337.07 mm^2.

To calculate the equivalent spring constant of the board, a different model must be used. As the board presents a certain thickness-to-length ratio, and the forces, which this component is subject, are not coaxial, the stainless steel board can be modeled as a simply supported Timoshenko beam.

The kinematic behavior of a straight Timoshenko beam under bending is illustrated in Figure 5. The results for this type of beam differ from the ones obtained through the Euler-Bernoulli model. Using Timoshenko beam model, the large angular deflections within the elastic limit are taken into account. The equivalent spring constant can be obtained from the relation between the applied load and resulting deflection, analogous to Hooke's law.

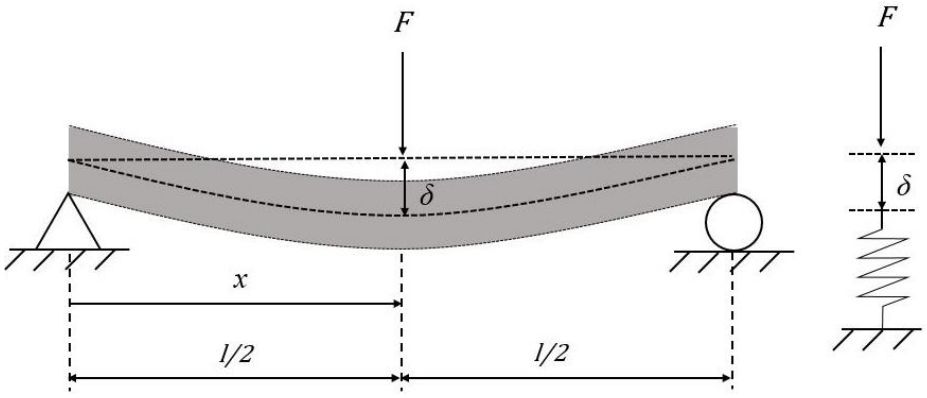

Figure 5. Schematic of a simply supported Timoshenko beam under a midspan concentrated load and equivalent spring model.

Mohyeddin and Fereidoon (2013) obtained an analytical solution for simply supported Timoshenko beams. The following equation describes the equivalent spring constant for the board:

$$k_{plate} = \frac{48EI}{l^2\left[3 - 4\left(\frac{x}{l}\right)^2\right]x} \tag{11}$$

where *I* is the moment of inertia, *l*, the length of the beam and *x*, position in the *x* direction. Besides, the overall set up equivalent spring constant can be calculated by:

$$k_{equivalent} = \left(\sum_{i=1}^{n} \frac{1}{k_i} \right)^{-1} \tag{12}$$

where k_i is the spring constant. Figure 6 depicts a schematic of the equivalent spring association adopted model. The hypothesis that the overall stiffness of the components can be modelled as a series of compressive springs is valid as the force on the screws is the same as the force on the board and on the slab. The hypothesis for this approach on the stiffness of the clamped components is also suggested by Budynas and Nibsbett (2011).

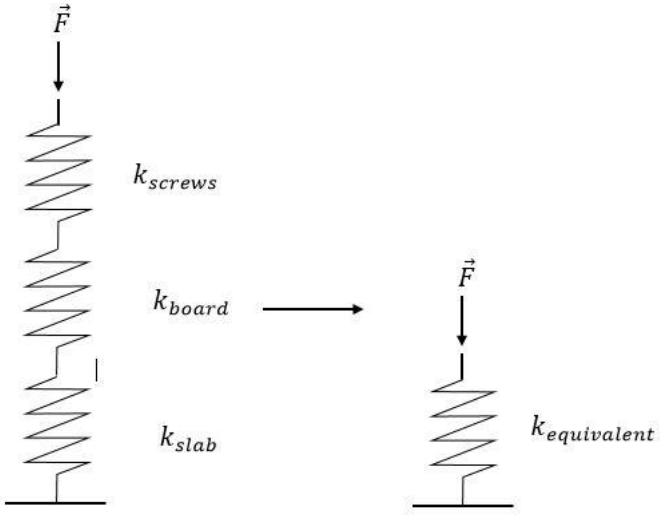

Figure 6. Equivalent spring association model.

Under the hypothesis that the force distribution is uniform along the affected area and that the stainless steel boards stay perfectly in parallel position during the bounding process, the pressure among the set up boards can be calculated considering the different material dilatation, using the Hooke's law:

$$F = k_{equivalent} \delta_{net} \tag{13}$$

where F is the force due to the deformation, δ_{net} is the net deformation and δ_{slab}, δ_{board} and δ_{screw} are the slab, board and screw dilatations, respectively. Actually, the screw dilatation is considered the maximum thermal dilation of the assembly. Therefore, the net deformation is assumed as the difference between the dilatation of the aluminum slabs and stainless steel boards *versus* that of the carbon steel screws, resulting in the expression:

$$\delta_{net} = \delta_{slab} + \delta_{board} - \delta_{screws} \tag{14}$$

As it was mentioned previously, the Young's Moduli change with the temperature. The behavior of the Young's Moduli (measured is *MPa*) for ferritic (carbon steel) and for austenitic (stainless steel), as obtained from AISI, is given by:

$$E_{CarbonSteel}(T)_{20<\Delta T<482} = -74.46T + 208289.18 \tag{15}$$

$$E_{CarbonSteel}(T)_{482<\Delta T<550} = -304.63T + 319232.79 \tag{16}$$

$$E_{StainlessSteel}(T) = -80.56T + 194611.11 \tag{17}$$

It is interesting to note that the Young's Modulus of the carbon steel experiences a sharp decline after a certain temperature. The behavior for the Young's Modulus for aluminum, on other hand, is (Summers *et al.*, 2015):

$$E_{Al}(T) = -120.83T + 70416.67 \tag{18}$$

With the net deformation and equivalent spring module, it is possible to calculate the resulting force. Figure 7 illustrates the variation of the set up pressure as a function of temperature.

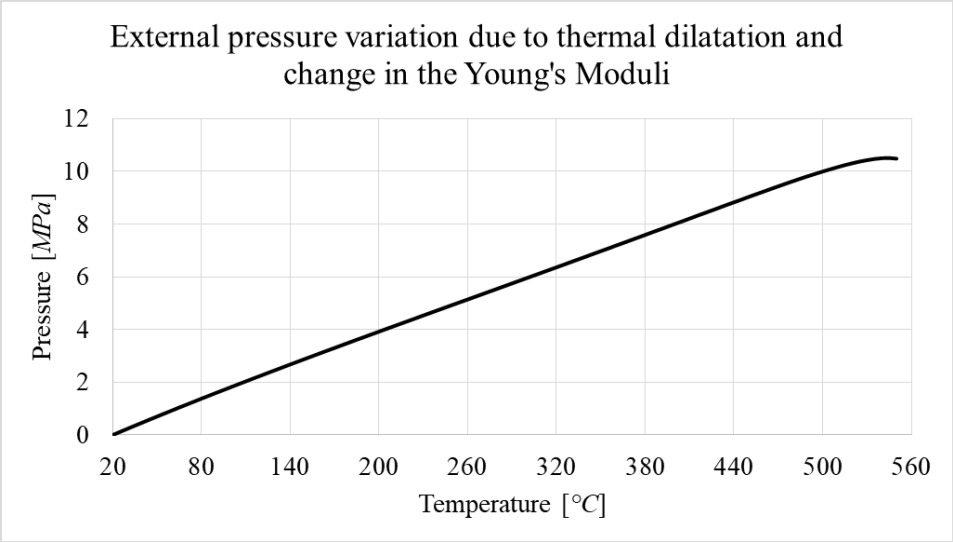

Figure 7. External pressure variation due to thermal dilatation and change in the Young's Moduli.

As predicted, pressure increases with the temperature in an almost linear fashion. However, it is interesting to note in this figure that, after a certain temperature, the device pressure starts to decline. This effect is mostly due the change on the Young's Modulus of the carbon steel. Actually, as one can see from equations 15 and 16, there is a considerable difference between the angular coefficients of the two equations. The decline of the Young's Modulus of the carbon steel affects the equivalent spring element model (which schematic is shown in Figure 6) and this effect is dominant over the thermal expansion of the components, after a given temperature.

As stated by Timoshenko and Gere (1983), the basic differential equation that dictates the elastic deformation behavior of a beam is linear. As a practical consequence, solutions for different loading conditions can be superposed.

As previously stated, the stresses on the stainless steel boards (outer elements) of the device can be modelled using Timoshenko beam theory. Figure 8 depicts a schematic of the physical model adopted in this analysis. As a hypothesis, the pressure applied over the bounding material (aluminum slabs) is considered uniform.

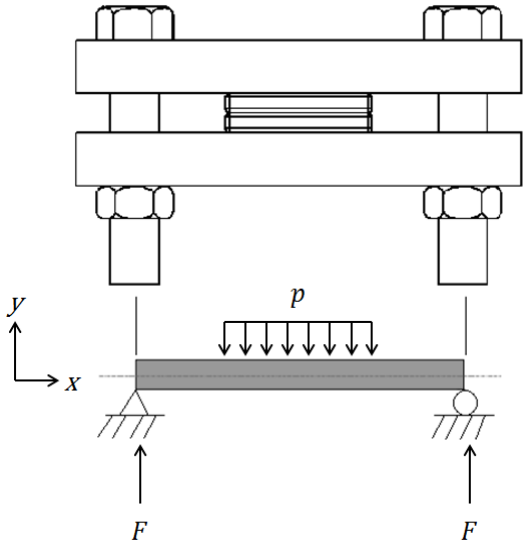

Figure 8. Physical model schematic for the pressure distribution over external boards.

Using the following equations, it is possible to calculate the stress distribution on the beam (Mohyeddin and Fereidoon, 2013):

$$\sigma = \frac{My}{I} \tag{19}$$

$$M(x) = \frac{F}{2}\left[x + \omega_0(x)\tan(\theta_0)\right] \tag{20}$$

$$\omega_0(x) = \frac{xFl^2\left[3 - 4\left(\frac{x}{l}\right)^2\right]}{48EI} \tag{21}$$

$$\theta_0(x) = \arctan\left\{\frac{Fl^2\left[1 - 4\left(\frac{x}{l}\right)^2\right]}{16EI}\right\} \tag{22}$$

where the symbols are explained Table 3.

Table 3. Physical meaning of the used symbols (equations 15 – 18)

Symbol	Physical meaning	Measurement Unit
σ	Axial tension on the beam	N/m^2
M	Bending moment on the beam	$N.m$
y	Position on the y direction relative to midsection	m
I	Moment of inertia of the beam	m^4
F	Force applied on the beam	N
x	Position on the x direction	m
ω_0	Displacement of the beam on the y direction	m
θ_0	Deflection angle at the end of the beam	°
l	Length of the beam	m

The middle of the beam ($x=l/2$) was chosen as the critical section, due to the symmetry of the load distribution. Three different positions for y were chosen, $h/2$, $h/4$ and $h/6$. These positions are depicted in Figure 9. The first value for y ($h/2$) is expected to experience the highest tension. The other two values were chosen to evaluate the stress distribution along the cross section of the beam.

The stress in these sections is calculated. The force applied on the beam is calculated with the hypothesis of uniform pressure distribution. The dilatation and the original pressure previously applied on the device are both taken into consideration of the stress analysis. Additionally, it was obtained from AISI, how the Yield Strength (0,2% offset) of austenitic stainless steels is influenced by temperature. The resulting curves are compared on Figure 10.

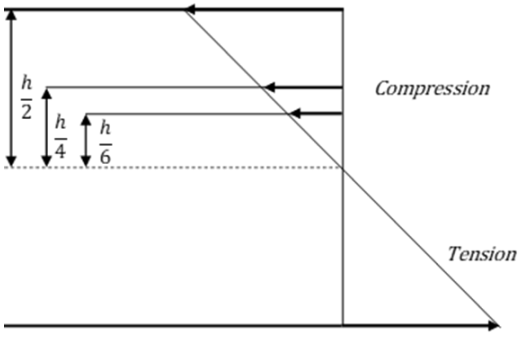

Figure 9. Stress distribution in a beam.

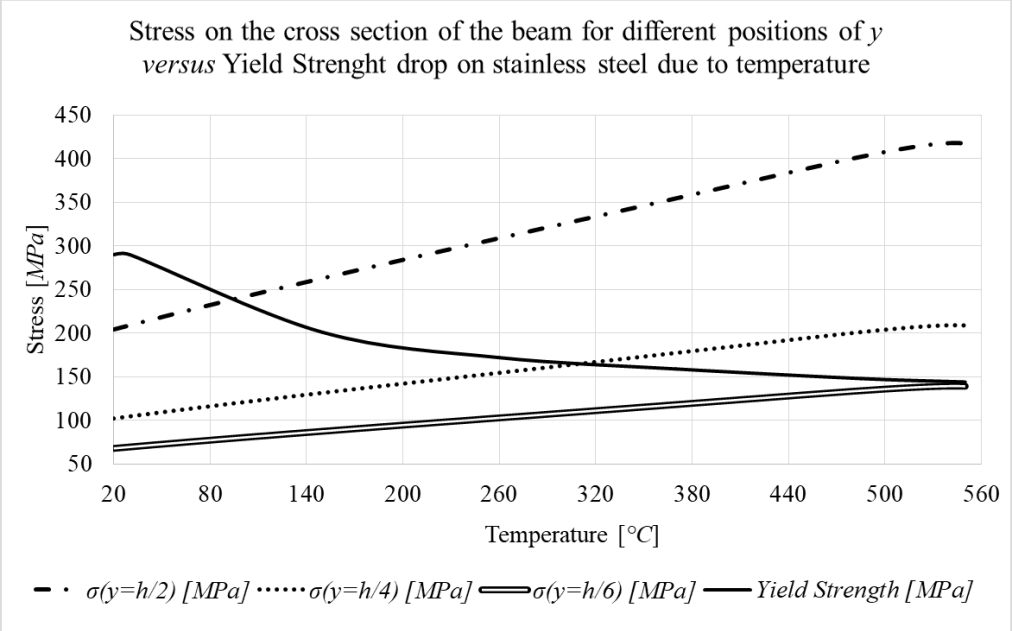

Figure 10. Stress on the beam *versus* Yield Strength drop on stainless steel due to temperature.

As it was expected, the stress variation (Figure 10) on the board follows the same trend as the pressure (Figure 7), even for different positions of *y*. For the three cases, it increases with the temperature and, after a certain point, starts to decline because of the change on the Young's Modulus of the carbon steel.

On the other hand, the Yield Strength declines almost linearly with the temperature to about 170°*C*. Afterwards, it presents a less prominent slope.

It should be noted that for *y=h/2*, approximately after 95°*C*, the stress on the middle section of the beam surpasses the Yield Strength of the material. This is also observed for *y=h/4*, at approximately *310°C*. This means that the deformation on the selected sections of the board would be both elastic and plastic in nature. However, for *y=h/6*, the stress is always in elastic regime. This shows that, while some sections of the board may experience plastic deformation, the component is not entirely out of the elastic regime. Therefore, it is expected that the device may present a residual tension after the diffusion bounding cycle.

3. RESULTS AND DISCUSSION

The required torque on the screws which would imposed the prescribed pressure on the system can be determined by Equation 1. The input parameters are: prescribed pressure and affected area, screw geometrical properties and the friction coefficients. The pressure distribution on the boards (stainless steel boards and aluminum slabs) is assumed uniform. Values for the friction coefficient (μ=0,15) are obtained from an industrial handbook specialized on tools and equipment (Atlas Copco, 2007). However, the materials mechanical and thermal properties are obtained from several different sources of literature, as a unique reliable source, regarding the behavior of materials when subject to different temperatures, was not found.

Several hypothesis were assumed for this analysis. One of the most important was that the net deformation on the device is the result of the sum of the dilatation of the aluminum slabs and of the stainless steel boards minus the dilatation of the carbon steel screws. This hypothesis establishes that the stainless steel screws are the most rigid components of the device. Observing the equivalent spring model and comparing the stiffness of the screws to that of other components, one can note that this hypothesis is actually consistent.

As shown in Figure 7, the variation of the set up pressure is a function of temperature, with the pressure applied on the set up increasing almost linearly. However, it is interesting to note that, after a certain temperature, the device pressure starts to decline. This effect is due the change on the Young's Modulus of carbon steel. Actually, as one can see from equations 15 and 16, there is a considerable difference between the angular coefficients of the two equations. However, as no deformation is considered for the screws (actually they provide pressure by their own), the actual deformation could smaller than predicted. This analysis is left as suggestion for future works. The present model, although simple, offers the possibility to outline of the experienced pressure change. Such information is useful in the initial phases of projects.

As observed on Figure 10, the critical section of the beam would present both elastic and plastic deformation. However, other regions of the boards may still be under the elastic deformation regime. If enough regions of the studied board present tensions smaller than the Yield strength, the geometrical integrity of the set up may still be preserved.

4. CONCLUSIONS

In this work, a solid mechanics study of a simple pressurizing system to be used in diffusion bonding is performed. The possibility of using simpler methods, especially in the initial phases of diffusion bonding process development, is appealing. One should note that hot press furnaces, which count with active control of temperature and pressure, can be considered the most appropriate devices for the process. However, the use of these devices has its technical restrains, as they present high rates of energy consumption, high operational costs, time-consuming cycles and are very sensitive to contamination.

A mathematical model to predict the stress within the set up components, due to the differential thermal expansion of the materials, was presented. While simple, it has as input data the thermal expansion coefficients, Young's moduli and Yield Strengths of different materials, due to the temperature levels. As a result, it is expected that the device may present a residual tension after the diffusion bounding cycle.

The main restrictions to the precision of the model lie in the assumptions that the deformation on the screws are only due to thermal dilatation. More sophisticated theories would give results closer to the reality of the problem. While the use of a numerical analysis software, which would automatically calculate the relation between stress and deformations, is a possibility, this method is not always readily available.

5. ACKNOWLEDGEMENTS

The authors would like to acknowledge the invaluable help from Professors Lauro Cesar Nicolazzi and Marcelo Krajnc Alves from the Department of Mechanical Engineering of the Federal University of Santa Catarina, who suggested the use of beam theory in the present work. Thanks is also due to Victor Matvienko for suggestions in the text.

6. REFERENCES

Atlas Copco, Tecnologia do aperto – guia de bolso, Atlas Copco (2007), 7.
American Iron and Steel Institute, High Temperature Characteristics of Stainless Steels, Nickel Development Institute
Budynas, R.G., Nibsbett, K. Shigley's Mechanical Engineering Design, McGraw-Hill (2011), 410-428.
Kazakov, N.F. Diffusion Bonding of Materials, Pergamon (1985), 10.
Matweb, 2017. "316 Stainless Steel, annealed sheet" 12 Set. 2017 < http://www.matweb.com>
Matweb, 2017. "AISI 1020 Steel, cold rolled" 12 Set. 2017 < http://www.matweb.com>
Matweb, 2017. "Aluminum, Al" 12 Set. 2017 < http://www.matweb.com>
Mohyeddin, A. Fereidoon, A. An analytical solution for large deflection problem of Timoshenko beams under three-point bending. *International Journal of Mechanical Sciences,* Vol. 78, p. 135-139.
Mortean, M.V.V.Desenvolvimento de tecnologias de recheios para trocadores de calor compactos soldados por difusão, Florianópolis, 2014, pp. 49-54.
Norton, R.L.Machine Design – An Integrated Approach, 2° Edition, Prendice Hall, 2007, 797.
Pavlova, N. Aplicação do processo de soldagem por difusão na união de componentes inoxidáveis para uso espacial, São José dos Campos, 2005, pp. 42.
Summers, P. T., Chen, Y., Rippe, C. M.m et al. Overview of aluminum alloy mechanical properties during and after fires, Fire Science Reviews, (2015).
Timoshenko, S. P., Gere, J. E. Mecânica dos Solidos, LCT (1983).

7. RESPONSIBILITY NOTICE

The authors are the only responsible for the printed material included in this paper.